Delft University of Technology

Delft Center for Systems and Control

Technical report 13-004

Optimal Trajectory Planning for Trains – A Pseudospectral Method and a Mixed Integer Linear Programming Approach*

Y. Wang, B. De Schutter, T. J. J. van den Boom, and B. Ning

To cite this work, please refer to the published version:

Y. Wang, B. De Schutter, T. J. J. van den Boom, and B. Ning, "Optimal trajectory planning for trains – A pseudospectral method and a mixed integer linear programming approach," *Transportation Research Part C*, vol. 29, pp. 97–114, Apr. 2013. doi:10.1016/j.trc.2013.01.007

Delft Center for Systems and Control
Delft University of Technology
Mekelweg 2, 2628 CD Delft
The Netherlands
phone: +31-15-278.24.73 (secretary)
URL: https://www.dcsc.tudelft.nl

* This report can also be downloaded via https://dspub.eu/13-004

Optimal Trajectory Planning for Trains — A pseudospectral method and a mixed integer linear programming approach

Yihui Wang[a,b,*], Bart De Schutter[a], Ton J.J. van den Boom[a], Bin Ning[b]

[a] *Delft Center for Systems and Control, Delft University of Technology, 2628 CD Delft, The Netherlands*
[b] *State Key Laboratory of Traffic Control and Safety, Beijing Jiaotong University, Beijing 100044, P.R. China*

Abstract

The optimal trajectory planning problem for train operations under constraints and fixed arrival time is considered. The varying line resistance, variable speed restrictions, and varying maximum traction force are included in the problem definition. The objective function is a trade-off between the energy consumption and the riding comfort. Two approaches are proposed to solve this optimal control problem. First, we propose to use the pseudospectral method, a state-of-the-art method for optimal control problems, which has not used for train optimal control before. In the pseudospectral method, the optimal trajectory planning problem is recast into a multiple-phase optimal control problem, which is then transformed into a nonlinear programming problem. However, the calculation time for the pseudospectral method is too long for the real-time application in an automatic train operation system. To shorten the computation time, the optimal trajectory planning problem is reformulated as a mixed-integer linear programming (MILP) problem by approximating the nonlinear terms in the problem by piecewise affine functions. The MILP problem can be solved efficiently by existing solvers that guarantee to return the global optimum for the proposed MILP problem. Simulation results comparing the pseudospectral method, the new MILP approach, and a discrete dynamic programming approach show that the pseudospectral method has the best control performance, but that if the required computation time is also take into consideration, the MILP approach yields the best overall performance. More specifically, for the given case study the control performance of the pseudospectral approach is about 10% better than that of the MILP approach, and the computation time of the MILP approach is two to three orders of magnitude smaller than that of the pseudospectral method and the discrete dynamic programming approach.

Keywords: trajectory planning, train operation, MILP, pseudospectral method

1. Introduction

Nowadays, a number of high-speed lines and dedicated urban rapid transit railway systems with short headways are operated with a high degree of automation (Hansen and Pachl, 2008).

*Corresponding author. Tel:+31 1527 82725; Fax:+31 1527 86679.
Email addresses: yihui.wang@tudelft.nl (Yihui Wang), b.deschutter@tudelft.nl (Bart De Schutter), a.j.j.vandenboom@tudelft.nl (Ton J.J. van den Boom), bning@bjtu.edu.cn (Bin Ning)

This requires an advanced train control system to fulfill safety and operational requirements, such as the European Train Control System, which includes the equipment on board of the trains as well as in the control center (Midya and Thottappillil, 2008). An advanced train control system enables the energy-efficient driving of trains, which becomes more and more important because of the rising energy prices and environmental concerns (Liu and Golovicher, 2003). The automatic train operation (ATO) subsystem of the advanced train control system drives the train according to an optimal trajectory and recalculates it when the operational conditions change (Peng, 2008). Therefore, it is important to design an efficient algorithm to find the optimal speed-position reference trajectory. The present paper proposes two approaches to determine the optimal trajectory, viz. the pseudospectral method and the mixed-integer linear programming approach.

In fact, the optimal control problem of train operations was solved firstly by applying the maximum principle by Ichikawa (1968). From the point view of optimal control, there are three basic numerical approaches for solving the optimal control problem: dynamic programming, indirect methods, and direct methods (Dielh et al., 2006). In the following, we will briefly present the research about the optimal control of trains in the literature for each of these three categories.

Dynamic programming simplifies a complicated problem by breaking it down into simpler subproblems in a recursive manner. The result obtained by the calculation is in the form of a feedback control law in tabular form. Franke et al. (2002) solved the optimal control problem by discrete dynamic programming and compared the results with those of sequential quadratic programming. They concluded that discrete dynamic programming deals better with the nonlinear optimal problem. Ko et al. (2004) also applied dynamic programming to optimize the optimal reference trajectory. The original problem is then transformed into a multi-stage decision process and can be solved in an acceptable time with their improvements. It is known that approximations need to be made, usually by discretization, when dynamic programming is applied to discrete-time systems with continuous state spaces (Dielh et al., 2006). This discretization leads to the "curse of dimensionality", which means exponential growth of the computation cost with respect to the dimension of the state space.

In an indirect method, the calculus of variations is used to obtain the first-order necessary conditions for optimality (Bryson and Ho, 1975; Pontryagin, 1962). A Hamiltonian boundary-value problem results from these necessary conditions. For a train with discrete control inputs, i.e. the traction/braking force can only take some discrete values, Howlett (2000) used the Karush-Kuhn-Tucker condition to determine the optimal switching times, for a given fixed discrete-valued control sequence. For a train with continuous control inputs, Howlett (1990) simplified the analysis by using Pontryagin's principle to reformulate the problem as a finite-dimensional constrained optimization problem where the unknown switching times are the variables. Later on, Khmelnitsky (2000) gave a comprehensive analysis of the optimal trajectory planning problem with a continually varying gradient and speed restrictions. The maximum principle was applied to obtain optimal operation regimes (i.e. maximum traction, cruising, coasting, and maximum braking) and their sequences. The drawback of indirect methods is that the boundary-value problem is often difficult to solve due to strong nonlinearity and instability.

In a direct method, the continuous-time optimal control problem is transformed into a nonlinear programming problem (Bettes, 2001). The resulting nonlinear programming problem is then solved by variants of well-developed algorithms, such as SNOPT (Gill et al., 2002) and IPOPT (Wächter and Biegler, 2006). Direct methods can easily handle inequality constraints on states and inputs (Dielh et al., 2006). Over the last decade, a particular class of direct meth-

ods, called pseudospectral methods, have risen to prominence in the numerical optimal control area (Elnagar et al., 1995). Pseudospectral methods were researched widely in the 1970s for solving partial differential equations (PDEs) in fluid dynamics (Canuto et al., 1988). Later on, they became an important methodology for the numerical solution of PDEs. From the 1990s on, pseudospectral methods were applied to solving optimal control problems (Gong et al., 2007), such as orbit transfers, lunar guidance, magnetic control. Recently, the scope of application has been broadened as a result of significant progress in large-scale computation. However, to the authors' best knowledge, pseudospectral methods have not been applied to trajectory planning of trains. Therefore, the pseudospectral method is used for the first time to solve the train trajectory planning problem in this paper.

On the other hand, multi-parametric quadratic programming is used in (Vašak et al., 2009) to calculate the optimal control law for train operations. The nonlinear train model with quadratic resistance is approximated by a piecewise affine function. Inspired by (Vašak et al., 2009), in Wang et al. (2011) we proposed to solve the optimal trajectory problem as a mixed integer linear programming (MILP) problem, which can be solved efficiently using existing commercial and free solvers (Linderoth and Ralphs, 2005; Atamtürk and Savelsbergh, 2005). In the current paper, the MILP approach is extended in the following three aspects: we now allow different coefficients for the piecewise function for each space interval, we also approximate the nonlinear maximum traction force by piecewise affine functions, and we consider a more realistic model for the line resistance. The performance of the pseudospectral method and the MILP approach is compared with the discrete dynamic programming approach proposed in (Franke et al., 2002). Franke et al. (2002) concluded that the performance of the discrete dynamic programming approach is better than the sequential quadratic programming approach and the coasting strategy obtained by the maximum principle. Therefore, we have selected the discrete dynamic programming approach as the third approach for the comparison of the case study.

The remainder of this paper is structured as follows. In Section 2 the nonlinear model of train operations is presented and the optimal trajectory planning problem is formulated. In Section 3 the optimal trajectory planning problem is recast as an multi-phase optimal control problem, which can be solved by the pseudospectral method. In Section 4 the nonlinear train model is formulated as a mixed logical dynamic model by approximating the nonlinear terms by piecewise functions and the optimal control problem is recast as an MILP problem. Section 5 illustrates with a case study how to calculate the optimal reference trajectory by the pseudospectral method and the MILP approach and it also compares these two approaches with the discrete dynamic programming approach. We conclude with a short discussion of some topics for future work in Section 6.

2. Problem description

2.1. Train Model

In the literature on train optimal control, usually the mass-point model of train is used (Franke et al., 2003). The motion of a train can then be described by the following simple continuous-time model (Liu and Golovicher, 2003):

$$m\rho\frac{\mathrm{d}v}{\mathrm{d}t} = u(t) - R_{\mathrm{b}}(v) - R_{\mathrm{l}}(s,v), \tag{1}$$

$$\frac{\mathrm{d}s}{\mathrm{d}t} = v, \tag{2}$$

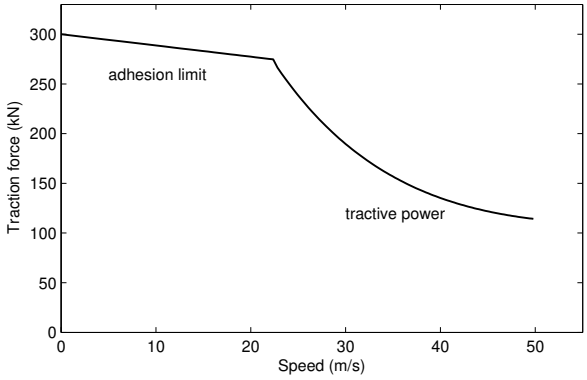

Figure 1: Maximum traction force in dependency of train speed

where m is the mass of the train, ρ is a factor to consider the rotating mass (Hansen and Pachl, 2008), v is the velocity of the train, s is the position of the train, u is the control variable, i.e. the traction or braking force, which is bounded by the maximum traction force $u_{\max}$ and the maximum braking force $u_{\min}$, $u_{\min} \leq u \leq u_{\max}$, $R_{\mathrm{b}}(v)$ is the basic resistance including roll resistance and air resistance, and $R_{\mathrm{l}}(s,v)$ is the line resistance caused by track grade, curves, and tunnels.

The maximum traction force $u_{\max}$ is often considered as constant in the literature (Howlett, 2000). However, in reality it is a function of the velocity v. Due to the maximum adhesion and the characteristics of the power equipment (Hansen and Pachl, 2008), the diagram of the maximum traction force $u_{\max}(v)$ normally looks like the one shown in Figure 1 (Hansen and Pachl, 2008). This diagram is described as a group of hyperbolic or parabolic formulas in (Hansen and Pachl, 2008), where each formula approximates the actual traction force for a certain speed interval. For example, if the train speed v belongs to interval $[v_j, v_{j+1}]$, then the maximum traction force can be written as

$$u_{\max}(v) = c_{1,j} + c_{2,j}v + c_{3,j}v^2, \quad v \in [v_j, v_{j+1}], \tag{3}$$

or

$$u_{\max}(v) = c_{\mathrm{h},j}/v, \; v \in [v_j, v_{j+1}], \text{ for } j = 1, 2, \cdots, M-1 \tag{4}$$

where v_j, v_{j+1}, $c_{1,j}$, $c_{2,j}$, $c_{3,j}$, and $c_{\mathrm{h},j}$ are determined by the characteristics of the train.

According to the arguments for the maximum braking force given in (Hansen and Pachl, 2008), the full braking effort is reserved for an emergency stop. Under normal circumstances the train driver or automatic train operation system brakes in a comfort mode, where the maximum force for the service breaking is 0.75 times that of the emergency braking, i.e. the full braking effort. On the other hand, the braking effort (including the maximum braking effort) is considered as constant by some common safety systems, such as the European Train Control System and the German continuous train control system (Hansen and Pachl, 2008). Therefore, the maximum force for service braking is taken to be constant in this paper.

In practice, according to the Strahl formula (Rochard and Schmid, 2000) the basic resistance $R_{\mathrm{b}}(v)$ can be described as

$$R_{\mathrm{b}}(v) = m(a_1 + a_2 v^2),$$

where the coefficients a_1 and a_2 depend on the train characteristics and the wind speed, which can be calculated from the data known about the train.

The line resistance $R_l(s,v)$ caused by track slope, curves, and tunnels can be described by (Mao, 2008)

$$R_l(s,v) = mg\sin\alpha(s) + f_c(r(s)) + f_t(l_t(s),v), \tag{5}$$

where g is the gravitational acceleration, $\alpha(s)$, $r(s)$, and $l_t(s)$ are the slope, the radius of the curve, and the length of the tunnel along the track, respectively. The curve resistance $f_c(\cdot)$ and the tunnel resistance $f_t(\cdot)$ are given by empirical formulas. An example of such an empirical formula of the curve resistance is Roeckl's formula (Huerlimann and Nash, 2003):

$$f_c(r(s)) = \frac{6.3}{r(s)-55}m \quad \text{for} \quad r(s) \geq 300\,\text{m},$$

$$f_c(r(s)) = \frac{4.91}{r(s)-30}m \quad \text{for} \quad r(s) < 300\,\text{m}.$$

When running in tunnels, the train experiences a higher air resistance that depends on the tunnel form, the smoothness of tunnel walls, the exterior surface of the train, and so on. An example of an expression for the tunnel resistance is as follows (Huerlimann and Nash, 2003; Gao, 2008). If there is a limiting gradient[1] in the tunnel, then an empirical formula for the tunnel resistance is

$$f_t(l_t(s),v) = 1.296\cdot 10^{-9} l_t(s) m g v^2.$$

If there does not exist a limiting gradient, the tunnel resistance can be calculated by the following empirical formula:

$$f_t(l_t(s),v) = 1.3\cdot 10^{-7} l_t(s) m g.$$

For the tracks outside the tunnels, the tunnel resistance is equal to zero.

2.2. Optimal Control Problem

As stated in (Liu and Golovicher, 2003), reference trajectory planning for trains can be formulated as an optimal control problem. The traction or braking force u then is the control variable. The state variables are the train position s and speed v. The objective function to be minimized could be the trip time, the energy consumption for a given trip time, or the total operation cost (a weighted sum of energy consumption and trip time). In this paper, we consider the objective criterion as the energy consumption in a fixed time span $[0,T]$ with T determined by a fixed or a flexible timetable (Hansen and Pachl, 2008; D'Ariano et al., 2008), or being the result of a rescheduling operation of railway traffic after disturbances (Krasemann, 2012). In addition, the riding comfort is considered, which is expressed as a function of the change of the control variable u, since reducing the number of transitions and the rate of change of u may improve passenger comfort (Chang and Xu, 2000). The objective function can thus be written as:

$$J = \int_0^T \left(u(t)\cdot v(t) + \lambda \cdot \left| \frac{\mathrm{d}u(t)}{\mathrm{d}t} \right| \right) \mathrm{d}t \tag{6}$$

[1] A limiting gradient is defined as the maximum railway gradient that can be climbed without the help of a second power unit.

where J is the weighted integral of the energy consumption and riding comfort and λ is the weight. This function will be minimized subject to the train dynamics (1) and (2), the constraints

$$u_{\min} \leq u(t) \leq u_{\max}(v) \tag{7}$$

$$0 \leq v(t) \leq V_{\max}(s) \tag{8}$$

and the boundary conditions

$$s(0) = s_{\text{start}}, \;\; v(0) = v_{\text{start}}, \tag{9}$$

$$s(T) = s_{\text{end}}, \;\; v(T) = v_{\text{end}}, \tag{10}$$

where the maximum allowable velocity $V_{\max}(s)$ depends on the train characteristics and the line conditions, and as such it is usually a piecewise constant function of the coordinate s (Liu and Golovicher, 2003; Khmelnitsky, 2000); s_{start} and v_{start} are the position and the velocity at the beginning of the route; s_{end} and v_{end} are the position and the velocity at the end of the route.

As proposed in some previous works (Liu and Golovicher, 2003; Franke et al., 2003; Khmelnitsky, 2000; Howlett, 2000), it is better to choose the position s as an independent variable rather than the time t. On the one hand, the choice of the position s as the independent variable will simplify the consideration of track-related data, such as line resistance and speed limits. On the other hand, the analytical and numerical study of the optimal control problem will be significantly simplified then. Furthermore, Khmelnitsky (2000) chose the total energy of the train and time t as states where the total energy includes kinetic and potential energy. Similarly, Franke et al. (2003) used kinetic energy per mass unit and time as states. The choice of kinetic energy instead of speed v will facilitate the study of the optimal control problem, because this choice eliminates some (but not all) of the model nonlinearities. Therefore, we also choose kinetic energy per mass unit $\tilde{E} = 0.5v^2$ and time t as states, and the position s as the independent variable. The continuous-time model (1) and (2) can then be rewritten as the following continuous-space model [2]:

$$m\rho \frac{\mathrm{d}\tilde{E}}{\mathrm{d}s} = u(s) - R_{\text{b}}(\sqrt{2\tilde{E}}) - R_{\text{l}}(s, v), \tag{11}$$

$$\frac{\mathrm{d}t}{\mathrm{d}s} = \frac{1}{\sqrt{2\tilde{E}}}. \tag{12}$$

The optimal control problem corresponding to (6)-(10) can be stated as: minimize the following objective function

$$J = \int_{s_{\text{start}}}^{s_{\text{end}}} \left(u(s) + \lambda \cdot \left| \frac{\mathrm{d}u(s)}{\mathrm{d}s} \right| \right) \mathrm{d}s \tag{13}$$

subject to the model (11) and (12), the constraints

$$u_{\min} \leq u(s) \leq u_{\max}(v), \tag{14}$$

$$0 \leq \tilde{E}(s) \leq \tilde{E}_{\max}(s), \tag{15}$$

[2] The transformation from $\frac{\mathrm{d}v}{\mathrm{d}t}$ to $\frac{\mathrm{d}\tilde{E}}{\mathrm{d}s}$ goes as follows:

$$\frac{\mathrm{d}v}{\mathrm{d}t} = \frac{\mathrm{d}v}{\mathrm{d}s}\frac{\mathrm{d}s}{\mathrm{d}t} = v\frac{\mathrm{d}v}{\mathrm{d}s} = \frac{\mathrm{d}\tilde{E}}{\mathrm{d}s}$$

where $\tilde{E} = 0.5v^2$.

and the boundary conditions,

$$\tilde{E}(s_{\text{start}}) = \tilde{E}_{\text{start}}, \;\; \tilde{E}(s_{\text{end}}) = \tilde{E}_{\text{end}}, \tag{16}$$

$$t(s_{\text{start}}) = 0, \;\; t(s_{\text{end}}) = T, \tag{17}$$

where $\tilde{E}_{\max}(s) = 0.5V_{\max}^2(s)$, $\tilde{E}_{\text{start}} = 0.5v_{\text{start}}^2$, and $\tilde{E}_{\text{end}} = 0.5v_{\text{end}}^2$. An assumption should be noted for the above equations. It is assumed that the unit kinetic energy $\tilde{E}(s)$ satisfies $\tilde{E}(s) \geq E_{\min} > 0$ with $E_{\min}$ a small positive number, which means the train's speed is always strictly larger than zero, i.e. the train travels nonstop. Khmelnitsky (2000) states that this assumption is not restrictive in practice for two reasons. First, the speed of the initial start and the terminal stop can be approximated by small nonzero velocities. Second, stops at an intermediate point of the trip will in principle not be planned deliberately in the optimal control design for a single train's operation.

Different types of rolling stock can be modeled by the mass-point model, whose parameters, such as mass, maximum traction force, and resistance coefficients, may vary according to different types of rolling stock. The existing infrastructure of tracks can be described accurately by using the line resistance (5), which includes track slope, curves, tunnels. In addition, the signaling aspects and the disturbances caused by other trains are assumed to be taken care of by a lower control level. Furthermore, different train categories (high speed trains, regional and intercity trains, freight trains) can be handled in a higher control level by timetable design, which specifies different running times and dwell times for each train. The approaches proposed in this paper can then be applied to obtain the optimal trajectory for each trip between two stations to save energy and ensure the passenger comfort based on the given timetable.

2.3. An assumption about the line resistance

The line resistance $R_{\text{l}}(s,v)$ caused by track slope, curves, and tunnels is a nonlinear function of the train's position and speed. In order to simplify the consideration of the line resistance, we rewrite $R_{\text{l}}(s,v)$ in (5) as

$$R_{\text{l}}(s,v) = \tilde{R}_{\text{l}}(s) + a_{\text{t}}(s)v^2, \tag{18}$$

where $\tilde{R}_{\text{l}}(s)$ are the terms that do not depend on the train's speed. In the sequel of this paper, $\tilde{R}_{\text{l}}(s)$ and $a_{\text{t}}(s)$ are assumed to be piece-wise constant functions, which can be written as

$$\begin{aligned} \tilde{R}_{\text{l}}(s) &= \tilde{R}_{\text{l}}^{(i)} \quad \text{for} \quad s \in [s_0^{(i)}, s_{\text{f}}^{(i)}], \\ a_{\text{t}}(s) &= a_{\text{t}}^{(i)} \quad \text{for} \quad s \in [s_0^{(i)}, s_{\text{f}}^{(i)}], \end{aligned} \tag{19}$$

for $i = 1,2,\cdots,N_{\text{R}}$, where N_{R} is the number of the piece-wise constant subfunctions, $s_0^{(1)} = s_{\text{start}}$ is the position at the beginning of the route, $s_{\text{f}}^{(N_{\text{R}})} = s_{\text{end}}$ is the position at the end of the route, and $s_0^{(i+1)} = s_{\text{f}}^{(i)}$ for $i = 1,2,\cdots,N_{\text{R}}-1$. Therefore, the line resistance can be written as

$$R_{\text{l}}(s,v) = \tilde{R}_{\text{l}}^{(i)} + a_{\text{t}}^{(i)}v^2, \quad \text{for} \quad s \in [s_0^{(i)}, s_{\text{f}}^{(i)}]. \tag{20}$$

3. Solution approach 1– Pseudospectral Method

3.1. Brief introduction to the pseudospectral method

The pseudospectral method directly formulates the original optimal control problem into an nonlinear programming problem, which can be solved numerically using a sparse nonlinear

programming solver to find approximate locally optimal solutions (Elnagar et al., 1995). It is shown by approximation theory and practice that the pseudospectral method is well suited for approximating smooth functions, integrations, and differentiations (Canuto et al., 1988). All those approximations are relevant to optimal control problems, e.g., the differential equations of the optimal control problem can then be approximated by algebraic equations (Ross and Fahroo, 2003). The main advantage of the pseudospectral method is the exponential rate of convergence and another advantage is that it is possible to achieve good accuracy with coarse grids (Canuto et al., 1988; Gong et al., 2008).

In the pseudospectral method, the state and control functions are approximated using orthogonal polynomials based on interpolation at orthogonal collocation points (Fornberg and Sloan, 1994), such as the commonly used Legendre-Gauss-Lobatto points, which are the roots of $(1-x^2)\frac{\mathrm{d}L_{\mathrm{N}(x)}}{\mathrm{d}x}$, where L_{N} is the Legendre polynomial of order N (Canuto et al., 1988). The derivative of the approximated state can be expressed in terms of the approximated state vector by using a differentiation matrix at the collocation points (Ross and Fahroo, 2004). When the optimal control problem includes discontinuities in states, controls, objective functional, or dynamic constraints, the pseudospectral method is employed in the form of a multiple-phase approach, where the problem is divided into a relatively small number of subintervals and global collocation is performed in each subinterval (Ross and Fahroo, 2004).

There exist several commercial and free packages that implement the pseudospectral method: PROPT (Rutquist and Edvall, 2008) and DIDO (Ross, 2004) are examples of commercial software that run under Matlab. A Matlab-based open source tool that uses the Gauss pseudospectral method is GPOPS (Rao et al., 2010). PSOPT is an open source optimal control package written in C++, including Legendre and Chebyshev pseudospectral discretizations (Becerra, 2010b).

3.2. Formulation of the optimal trajectory planning problem

We can reformulate the train trajectory planning problem (11)-(17) into the following general optimal control problem with N_{p} phases (Ross and Fahroo, 2004; Becerra, 2010a). It is worth to note that N_{p} is not equal to N_{R} of (19)-(20), but it will in general be larger. The objective function (13) to be minimized can be rewritten as

$$J=\sum_{i=1}^{N_{\mathrm{p}}}\left[\int_{s_0^{(i)}}^{s_{\mathrm{f}}^{(i)}}\left[u^{(i)}(s)+\lambda\left|\frac{\mathrm{d}u^{(i)}(s)}{\mathrm{d}s}\right|\right]\mathrm{d}s\right]. \tag{21}$$

Given that non-smoothness causes problems in nonlinear programming, a smooth version of the absolute value function can be written as

$$\left|\sigma\right|\approx\psi(\sigma)=\frac{\sigma^2}{\sqrt{\sigma^2+c^2}}, \tag{22}$$

where c is a constant deciding the smoothness of the function. Thus, the smooth objective function can be written as

$$J=\sum_{i=1}^{N_{\mathrm{p}}}\left[\int_{s_0^{(i)}}^{s_{\mathrm{f}}^{(i)}}\left[u^{(i)}(s)+\lambda\,\psi\Big(\frac{\mathrm{d}u^{(i)}(s)}{\mathrm{d}s}\Big)\right]\mathrm{d}s\right]. \tag{23}$$

The objective function (23) is subject to the differential constraints

$$\dot{x}^{(i)}(s)=\phi^{(i)}\big(x^{(i)}(s),u^{(i)}(s),s\big),\quad s\in[s_0^{(i)},s_{\mathrm{f}}^{(i)}], \tag{24}$$

where $x^{(i)}(s)$ is the state of the system in the ith phase, i.e., $x^{(i)}(s) = \begin{bmatrix} E^{(i)}(s) & t^{(i)}(s) \end{bmatrix}^T$, and the functions $\phi^{(i)}(\cdot)$ are defined by model equations (11)-(12) and the piece-wise line resistance (20). The path constraints of the optimal control problem are defined by (3), (4), and (14). Note that the path constraints caused by the maximum traction force are non-smooth. They can be approximated by smooth constraints by introducing a smooth version of the Heaviside function $H(\sigma)$, defined as $H(\sigma) = 1$, if $\sigma > 0$, and $H(\sigma) = 0$ otherwise (Kanwal, 1983). The approximation is implemented as

$$H(\sigma) \approx 0.5(1 + \tanh(\sigma/h)) \tag{25}$$

where $h > 0$ is a small real number. The path constraints can then be written as

$$h_{\mathrm{L}}^{(i)} \leq h^{(i)}\left(x^{(i)}(s), u^{(i)}(s), s\right) \leq h_{\mathrm{U}}^{(i)}, \quad s \in [s_0^{(i)}, s_{\mathrm{f}}^{(i)}]. \tag{26}$$

For the train trajectory planning problem, the initial position of the $(i+1)$th phase is equal to the final position of the ith phase, so one of the phase boundary constraints can be written as

$$s_0^{(i+1)} - s_{\mathrm{f}}^{(i)} = 0. \tag{27}$$

In addition, the states and control variable are continuous across the phase boundary, which can be written as

$$x(s_0^{(i+1)}) - x(s_{\mathrm{f}}^{(i)}) = 0, \tag{28}$$

$$u(s_0^{(i+1)}) - u(s_{\mathrm{f}}^{(i)}) = 0. \tag{29}$$

In general, phase boundary constraints (Betts, 1998; Becerra, 2010a) that link all the states and controls across the boundaries can be included in

$$\begin{aligned} \Psi_{\mathrm{L}} \leq \Psi(&x^{(1)}(s_0^{(1)}), u^{(1)}(s_0^{(1)}), x^{(1)}(s_{\mathrm{f}}^{(1)}), u^{(1)}(s_{\mathrm{f}}^{(1)}), s_0^{(1)}, s_{\mathrm{f}}^{(1)}, \\ &x^{(2)}(s_0^{(2)}), u^{(2)}(s_0^{(2)}), x^{(2)}(s_{\mathrm{f}}^{(2)}), u^{(2)}(s_{\mathrm{f}}^{(2)}), s_0^{(2)}, s_{\mathrm{f}}^{(2)}, \\ &\vdots \\ &x^{(N_{\mathrm{p}})}(s_0^{(N_{\mathrm{p}})}), u^{(N_{\mathrm{p}})}(s_0^{(N_{\mathrm{p}})}), x^{(N_{\mathrm{p}})}(s_{\mathrm{f}}^{(N_{\mathrm{p}})}), u^{(N_{\mathrm{p}})}(s_{\mathrm{f}}^{(N_{\mathrm{p}})}), s_0^{(N_{\mathrm{p}})}, s_{\mathrm{f}}^{(N_{\mathrm{p}})}) \leq \Psi_{\mathrm{U}}. \end{aligned} \tag{30}$$

Note that (27)-(29) are special cases of (30) with $\Psi_{\mathrm{L},i} = \Psi_{\mathrm{U},i}$.

The bound constraints can be written as

$$\begin{aligned} u_{\mathrm{L}}^{(i)} \leq u^{(i)}(s) \leq u_{\mathrm{U}}^{(i)}, \quad s \in [s_0^{(i)}, s_{\mathrm{f}}^{(i)}], \\ x_{\mathrm{L}}^{(i)} \leq x^{(i)}(s) \leq x_{\mathrm{U}}^{(i)}, \quad s \in [s_0^{(i)}, s_{\mathrm{f}}^{(i)}]. \end{aligned} \tag{31}$$

This multiple-phase optimal control problem can be solved using the pseudospectral method. However, the computation of the pseudospectral method is in general too slow for the real-time application of ATO system. When the operational conditions (e.g. speed limits or trip time) change while the train is driving (e.g. due to an accident or bad weather conditions), the ATO system needs to recalculate the optimal trajectory. If the algorithm of the ATO system takes a large computation time to calculate the optimal trajectory, then it is too late for the train to react

timely. Therefore, in the next section we propose a more efficient approach, i.e. mixed integer linear programming (MILP) approach, to calculate the optimal trajectory.

It is worth to note that the optimal solution of the pseudospectral method satisfies the necessary (but not always sufficient) conditions of optimality (Rutquist and Edvall, 2008). So it is guaranteed that the returned solution cannot be improved by an infinitesimal change in the trajectory, but there may exist completely different trajectories that yield a better performance. On the contrary, an MILP problem can be solved efficiently by existing solvers that guarantee the global optimum for the proposed MILP problem.

4. Solution approach 2 – MILP approach

In Wang et al. (2011), the nonlinear model of the train is transcribed into a piecewise affine (PWA) model by approximating the nonlinear terms through PWA functions. Furthermore, the PWA model can then be formulated as a mixed logical dynamic (MLD) model by applying some transformation properties from Williams (1999). The original optimal control problem is then transformed into an MILP problem based on the MLD model. The line resistance is considered as a piecewise constant function in Wang et al. (2011), while in reality the train experiences a higher air resistance when running in tunnels. Therefore, in this paper the quadratic term of the velocity is included in the line resistance. In addition, the nonlinear function $f(E) = \frac{1}{2\sqrt{2E}}$ appearing in the time equation is approximated by a PWA function with 3 subfunctions in Wang et al. (2011). In order to achieve additional accuracy, we use different coefficients for each space interval. Furthermore, the maximum traction force is considered as a constant in Wang et al. (2011); however, in reality it is a nonlinear function of the velocity, which is approximated by a PWA function in this paper.

For the MILP approach, we split the position horizon $[s_{\text{start}}, s_{\text{end}}]$ into N intervals (with $N \geq N_{\text{R}}$) to get a discrete-space model similarly as the one in (Franke et al., 2003). We assume that the track and train parameters as well as traction or breaking force can be considered as constant in each interval $[s_k, s_{k+1}]$ with length $\Delta s_k = s_{k+1} - s_k$, for $k = 1, 2, \ldots, N$. Note that $s_1 = s_{\text{start}}$ and $s_{N+1} = s_{\text{end}}$. By redefining the discretization of the interval $[s_{\text{start}}, s_{\text{end}}]$ if necessary, we can assume without loss of generality that $\tilde{R}_{\text{l}}(s)$ and $a_{\text{t}}(s)$ (cf. Section 2.3) are of the following form:

$$\begin{aligned} \tilde{R}_{\text{l}}(s) &= \tilde{R}_{\text{l},k} \quad \text{for} \quad s \in [s_k, s_{k+1}], \\ a_{\text{t}}(s) &= a_{\text{t},k} \quad \text{for} \quad s \in [s_k, s_{k+1}]. \end{aligned}$$

for $k = 1, 2, \cdots, N$.

4.1. Transformation properties

First, we introduce three properties according to (Williams, 1999). Consider the statement $\tilde{f}(\tilde{x}) \leq 0$, where $\tilde{f} : \mathbb{R}^n \to \mathbb{R}$ is affine, $\tilde{x} \in \chi$ with $\chi \subset \mathbb{R}^n$ and let

$$\tilde{M} = \max_{\tilde{x} \in \chi} \tilde{f}(\tilde{x}), \; \tilde{m} = \min_{\tilde{x} \in \chi} \tilde{f}(\tilde{x}). \tag{32}$$

If we introduce the logical variable $\delta \in \{0, 1\}$, then the following equivalence holds:

$$[\tilde{f}(\tilde{x}) \leq 0] \Leftrightarrow [\delta = 1] \quad \text{is true iff} \quad \begin{cases} \tilde{f}(\tilde{x}) \leq \tilde{M}(1 - \delta) \\ \tilde{f}(\tilde{x}) \geq \varepsilon + (\tilde{m} - \varepsilon)\delta \end{cases} \tag{33}$$

where ε is a small positive number (typically the machine precision) that is introduced to transform a strict equality into a non-strict inequality, which fits the MLD and MILP frameworks (Bemporad and Morari, 1999).

The product of two logical variables $\delta_1\delta_2$ can be replaced by an auxiliary logical variable $\delta_3 = \delta_1\delta_2$, i.e. $[\delta_3 = 1] \leftrightarrow [\delta_1 = 1] \wedge [\delta_2 = 1]$, which is equivalent to

$$\begin{cases} -\delta_1 + \delta_3 \leq 0, \\ -\delta_2 + \delta_3 \leq 0, \\ \delta_1 + \delta_2 - \delta_3 \leq 1. \end{cases} \tag{34}$$

Moreover, the product $\delta\tilde{f}(\tilde{x})$ can be replaced by the auxiliary real variable $z = \delta\tilde{f}(\tilde{x})$, which satisfies $[\delta = 0] \Rightarrow [z = 0]$ and $[\delta = 1] \Rightarrow [z = \tilde{f}(\tilde{x})]$. Then $z = \delta\tilde{f}(\tilde{x})$ is equivalent to

$$\begin{cases} z \leq \tilde{M}\delta, \\ z \geq \tilde{m}\delta, \\ z \leq \tilde{f}(\tilde{x}) - \tilde{m}(1-\delta), \\ z \geq \tilde{f}(\tilde{x}) - \tilde{M}(1-\delta). \end{cases} \tag{35}$$

It is noted that (33), (34), and (35) yield linear inequalities since $\tilde{f}$ is affine.

4.2. The mixed logical dynamic (MLD) model

In the interval $[s_k, s_{k+1}]$, the differential equation of the kinetic energy (11) can now be rewritten as

$$\frac{\mathrm{d}\tilde{E}}{\mathrm{d}s} = \frac{1}{m\rho}u(k) - \frac{2(a_2 + a_{\mathrm{t},k})}{\rho}\tilde{E}(s) - \frac{1}{\rho}(a_1 + \tilde{R}_{1,k}),$$

where $u(k)$ is a constant in the interval $[s_k, s_{k+1}]$. By defining $\zeta = \frac{1}{m\rho}$, $\eta_k = -\frac{2(a_2+a_{\mathrm{t},k})}{\rho}$, $\gamma_k = -\frac{1}{\rho}(a_1 + \tilde{R}_{1,k})$, this equation can be rewritten as

$$\frac{\mathrm{d}\tilde{E}}{\mathrm{d}s} = \zeta u(k) + \eta_k\tilde{E}(s) + \gamma_k. \tag{36}$$

We have to solve this differential equation with initial condition $\tilde{E}(s_k) = E(k)$. For the sake of simplicity, we use $E(k)$ as a short-hand notation for $\tilde{E}(s_k)$ from now on. Then we obtain the following formula for $E(k+1)$:

$$E(k+1) = e^{\eta_k\Delta s_k}E(k) + (e^{\eta_k\Delta s_k} - 1)\frac{\zeta}{\eta_k}u(k) + (e^{\eta_k\Delta s_k} - 1)\frac{\gamma_k}{\eta_k}$$

with $E(1) = \tilde{E}_{\mathrm{start}}$ and $E(N+1) = \tilde{E}_{\mathrm{end}}$. Defining $a_k = e^{\eta_k\Delta s_k}$, $b_k = (e^{\eta_k\Delta s_k} - 1)\frac{\zeta}{\eta_k}$ and $c_k = (e^{\eta_k\Delta s_k} - 1)\frac{\gamma_k}{\eta_k}$, the above equation can be simplified as follows:

$$E(k+1) = a_kE(k) + b_ku(k) + c_k. \tag{37}$$

Note that this is an affine equation. As regards the differential equation of time (12), we approximate it by using a trapezoidal integration rule (Atkinson, 1978):

$$t(k+1) = t(k) + \frac{1}{2}\left(\frac{1}{\sqrt{2E(k)}} + \frac{1}{\sqrt{2E(k+1)}}\right)\Delta s_k \tag{38}$$

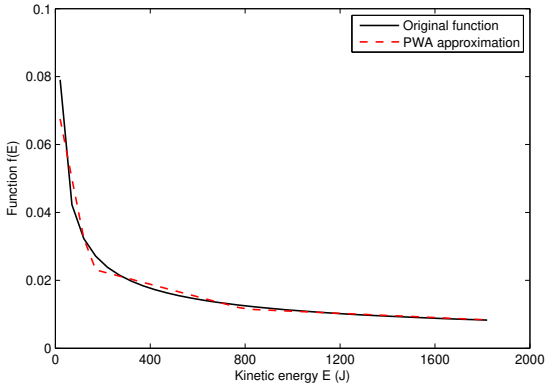

Figure 2: The PWA approximation of the nonlinear function $f(E)$

with $t(1) = 0$. In addition, the nonlinear part in this equation is approximated by a PWA function. There are various methods for approximating functions in a PWA way, see e.g., the overview by Azuma et al. (2010). In this paper, we first select the number of regions of the PWA function and then optimize the interval lengths and parameters of the affine functions using least-squares optimization, minimizing the squared difference between the original function and the approximation. Recall that $E_{\min}$ denotes the minimum kinetic energy. Define the maximum kinetic energy

$$E_{\max} = \max_{k=1,2,\ldots,N}(E_{\max}(k)) = \max_{k=1,2,\ldots,N}\left(\frac{1}{2}v_{\max}^2(k)\right).$$

In Wang et al. (2011), the nonlinear function $f(E) = \frac{1}{2\sqrt{2E}}$ is approximated over the interval $[E_{\min}, E_{\max}]$ by a PWA function with 3 affine subfunctions (shown as Figure 2) . However, the speed limit depends on the space interval, i.e. different space intervals may have different speed limit, which may be less than the overall maximum of the speed limit. Therefore, if we adapt these coefficients of PWA approximations depending on the space interval index k, i.e. we can have different PWA subfunctions for different space intervals within valid speed intervals. In this way the approximation error will be reduced. For example, if we consider an approximation using 3 affine subfunctions (cf. Figure 2), the PWA approximation[3] of the nonlinear function $f(E(k)) = \frac{1}{2\sqrt{2E(k)}}$ can be written as

$$f_{\text{PWA}}(E(k)) = \begin{cases} \alpha_{1,k}E(k) + \beta_{1,k} & \text{for } E_{0,k} \le E(k) \le E_{1,k}, \\ \alpha_{2,k}E(k) + \beta_{2,k} & \text{for } E_{1,k} \le E(k) \le E_{2,k}, \\ \alpha_{3,k}E(k) + \beta_{3,k} & \text{for } E_{2,k} \le E(k) \le E_{3,k}, \end{cases} \tag{39}$$

with $E_{0,k} = E_{\min}$ and $E_{3,k} = E_{\max}(k)$ for the interval $[s_k, s_{k+1}]$. Furthermore, the values of $E_{1,k}$ and $E_{2,k}$ are determined by the least-squares optimization.

Now the time dynamics (38) can be approximated as

$$t(k+1) = t(k) + (\alpha_{l,k}E(k) + \beta_{l,k} + \alpha_{m,k+1}E(k+1) + \beta_{m,k+1})\Delta s_k, \tag{40}$$

[3]The approximation error can be reduced by taking more regions.

when $E_{l-1,k} \leq E(k) \leq E_{l,k}$, $E_{m-1,k+1} \leq E(k+1) \leq E_{m,k+1}$, with $l,m \in \{1,2,3\}$.

Furthermore, the maximum traction force $u_{\max}$ is a nonlinear function of the velocity as we mentioned before, which can be reformulated as a nonlinear function of the kinetic energy. In a similar way as the approximation of the nonlinear function $f(E(k))$, we can obtain the PWA approximation of the maximum traction force. If we consider an approximation using[4] 3 affine subfunctions (cf. (39)), then the approximation can be written as

$$u_{\max,\mathrm{PWA}}(E(k)) = \begin{cases} \lambda_{1,k}E(k) + \mu_{1,k} & \text{for } E_{4,k} \leq E(k) \leq E_{5,k}, \\ \lambda_{2,k}E(k) + \mu_{2,k} & \text{for } E_{5,k} \leq E(k) \leq E_{6,k}, \\ \lambda_{3,k}E(k) + \mu_{3,k} & \text{for } E_{6,k} \leq E(k) \leq E_{7,k}, \end{cases} \tag{41}$$

with $E_{4,k} = E_{\min}$ and $E_{7,k} = E_{\max}(k)$ and where the values of $E_{5,k}$ and $E_{6,k}$ are decided by the approximation process.

The above PWA model with PWA constraints can be transformed into an MLD model by introducing some auxiliary logical variables (Bemporad and Morari, 1999). First consider (39). In order to transform this equation, we introduce auxiliary logical variables $\delta_1(k)$ and $\delta_2(k)$, defined as

$$\begin{aligned} [E(k) \leq E_{1,k}] &\Leftrightarrow [\delta_1(k) = 1], \\ [E(k) \leq E_{2,k}] &\Leftrightarrow [\delta_2(k) = 1]. \end{aligned} \tag{42}$$

Then we get

$$\begin{aligned} f_{\mathrm{PWA}}(E(k)) =& \delta_1(k)\delta_2(k)[\alpha_{1,k}E(k) + \beta_{1,k}] + (1-\delta_1(k))\delta_2(k)[\alpha_{2,k}E(k) + \beta_{2,k}] \\ &+ (1-\delta_1(k))(1-\delta_2(k))[\alpha_{3,k}E(k) + \beta_{3,k}]. \end{aligned} \tag{43}$$

Since the maximum and minimum values of $E(k)$ are $E_{\max}(k)$ and $E_{\min}$, according to the transformation property (33), the logical conditions (42) can be rewritten as linear inequalities. Furthermore, the auxiliary logical variable $\delta_3(k)$ is introduced to replace the product $\delta_1(k)\delta_2(k)$. The condition $\delta_3(k) = \delta_1(k)\delta_2(k)$ can be rewritten as a system of linear inequalities according to (34). By defining new auxiliary variables $z_1(k) = \delta_1(k)E(k)$, $z_2(k) = \delta_2(k)E(k)$, and $z_3(k) = \delta_3(k)E(k)$, which can be expressed as a system of linear inequalities according to (35), the function $f_{\mathrm{PWA}}(E(k))$ can be rewritten as

$$\begin{aligned} f_{\mathrm{PWA}}(E(k)) =& \begin{bmatrix} -\alpha_{3,k} & \alpha_{2,k} - \alpha_{3,k} & \alpha_{1,k} - \alpha_{2,k} + \alpha_{3,k} \end{bmatrix} \begin{bmatrix} z_1(k) & z_2(k) & z_3(k) \end{bmatrix}^T \\ &+ \begin{bmatrix} -\beta_{3,k} & \beta_{2,k} - \beta_{3,k} & \beta_{1,k} - \beta_{2,k} + \beta_{3,k} \end{bmatrix} \begin{bmatrix} \delta_1(k) & \delta_2(k) & \delta_3(k) \end{bmatrix}^T + \alpha_{3,k}E(k) + \beta_{3,k}, \end{aligned} \tag{44}$$

In order to deal with the PWA constraints of the maximum traction force (cf. (41)), an auxiliary logical variable $\delta_4(k)$ and $\delta_5(k)$ is introduced that defined by

$$\begin{aligned} [E(k) \leq E_{5,k}] &\Leftrightarrow [\delta_4(k) = 1], \\ [E(k) \leq E_{6,k}] &\Leftrightarrow [\delta_5(k) = 1]. \end{aligned} \tag{45}$$

Similar to (42), the logical conditions (45) can be recast as linear inequalities by applying transformation property (33). In addition, another binary variable $\delta_6(k)$ is introduced similarly as $\delta_3(k)$, and it is defined as $\delta_6(k) = \delta_4(k)\delta_5(k)$. Furthermore, auxiliary variables $z_4(k) =$

[4] For M affine subfunctions with $M > 3$ a similar procedure can be used.

$\delta_4(k)E(k)$, $z_5(k)=\delta_5(k)E(k)$, and $z_6(k)=\delta_6(k)E(k)$ are defined in order to write the constraints into a system of linear inequalities. The PWA constraints $u(k)\leq u_{\max,\mathrm{PWA}}(E(k))$ can then be written as

$$\begin{aligned}u(k)\leq&\begin{bmatrix}-\lambda_{3,k} & \lambda_{2,k}-\lambda_{3,k} & \lambda_{1,k}-\lambda_{2,k}+\lambda_{3,k}\end{bmatrix}\begin{bmatrix}z_4(k) & z_5(k) & z_6(k)\end{bmatrix}^T\\&+\begin{bmatrix}-\mu_{3,k} & \mu_{2,k}-\mu_{3,k} & \mu_{1,k}-\mu_{2,k}+\mu_{3,k}\end{bmatrix}\begin{bmatrix}\delta_4(k) & \delta_5(k) & \delta_6(k)\end{bmatrix}^T+\lambda_{3,k}E(k)+\mu_{3,k}.\end{aligned}\tag{46}$$

Now the dynamics of the system can be rewritten as the following MLD model

$$x(k+1)=A_kx(k)+B_ku(k)+C_{1,k}\delta(k)+C_{2,k}\delta(k+1)+D_{1,k}z(k)+D_{2,k}z(k+1)+e_k,\tag{47}$$

where

$$\begin{aligned}&x(k)=\begin{bmatrix}E(k) & t(k)\end{bmatrix}^T, A_k=\begin{bmatrix}a_k & 0\\ \Delta s_k(\alpha_{3,k}+a_k\alpha_{3,k+1}) & 1\end{bmatrix}, B_k=\begin{bmatrix}b_k\\ \Delta s_k\alpha_{3,k+1}b_k\end{bmatrix},\\
&C_{1,k}=\Delta s_k\begin{bmatrix}0 & 0 & 0 & 0 & 0 & 0\\ -\beta_{3,k} & \beta_{2,k}-\beta_{3,k} & \beta_{1,k}-\beta_{2,k}+\beta_{3,k} & 0 & 0 & 0\end{bmatrix},\\
&C_{2,k}=\Delta s_k\begin{bmatrix}0 & 0 & 0 & 0 & 0 & 0\\ -\beta_{3,k+1} & \beta_{2,k+1}-\beta_{3,k+1} & \beta_{1,k+1}-\beta_{2,k+1}+\beta_{3,k+1} & 0 & 0 & 0\end{bmatrix},\\
&D_{1,k}=\Delta s_k\begin{bmatrix}0 & 0 & 0 & 0 & 0 & 0\\ -\alpha_{3,k} & \alpha_{2,k}-\alpha_{3,k} & \alpha_{1,k}-\alpha_{2,k}+\alpha_{3,k} & 0 & 0 & 0\end{bmatrix},\\
&D_{2,k}=\Delta s_k\begin{bmatrix}0 & 0 & 0 & 0 & 0 & 0\\ -\alpha_{3,k+1} & \alpha_{2,k+1}-\alpha_{3,k+1} & \alpha_{1,k+1}-\alpha_{2,k+1}+\alpha_{3,k+1} & 0 & 0 & 0\end{bmatrix},\\
&\text{and}\quad e_k=\begin{bmatrix}c_k\\ \Delta s_k(\alpha_{3,k+1}c_k+\beta_{3,k}+\beta_{3,k+1})\end{bmatrix}.\end{aligned}$$

The MLD model (47) is subject to the linear constraints of the form (33), (34), and (35) resulting from the transformation as well as the upper bound and lower bound constraints for $E(k)$, $t(k)$, and $u(k)$. All these constraints can be written more compactly as

$$R_{1,k}\delta(k)+R_{2,k}\delta(k+1)+R_{3,k}z(k)+R_{4,k}z(k+1)\leq R_{5,k}u(k)+R_{6,k}x(k)+R_{7,k},\tag{48}$$

with appropriately defined coefficient matrices $R_{i,k}$, for $i=1,2,\ldots,7$.

The objective function (13) can be discretized as

$$J=\sum_{k=1}^{N}u(k)\Delta s_k+\sum_{k=1}^{N-1}\lambda\,|\Delta u(k)|,\tag{49}$$

where $\Delta u(k)=u(k+1)-u(k)$. We introduce a new variable $\omega(k)$ to deal with the absolute value of $\Delta u(k)$, and we add the linear inequalities:

$$\begin{aligned}\omega(k)&\geq u(k+1)-u(k),\\ \omega(k)&\geq u(k)-u(k+1).\end{aligned}\tag{50}$$

Since $\lambda>0$, minimizing (49) is equivalent to minimizing

$$\tilde{J}=\sum_{k=1}^{N}u(k)\Delta s_k+\sum_{k=1}^{N-1}\lambda\,\omega(k).\tag{51}$$

subject to (50). Indeed, it is easy to verify that when we minimize the objective function (51) subject to (50), the optimal value of $\omega(k)$ will be equal to $|\Delta u(k)|$, so (49) will also be minimized.

4.3. The mixed linear programming problem (MILP)

Now the optimal control problem can be recast as a mixed integer linear programming (MILP) problem, where some of decision variables are binary (i.e. $\tilde{\delta}$) and some are real variables (i.e. $\tilde{u}, \tilde{\omega}, \tilde{z}$) with

$$\tilde{u} = \begin{bmatrix} u(1) \\ u(2) \\ \vdots \\ u(N) \end{bmatrix}, \tilde{\delta} = \begin{bmatrix} \delta(1) \\ \delta(2) \\ \vdots \\ \delta(N+1) \end{bmatrix}, \tilde{z} = \begin{bmatrix} z(1) \\ z(2) \\ \vdots \\ z(N+1) \end{bmatrix}, \tilde{\omega} = \begin{bmatrix} \omega(1) \\ \omega(2) \\ \vdots \\ \omega(N-1) \end{bmatrix},$$

Furthermore, if we define $\tilde{V} = \begin{bmatrix} \tilde{u}^T & \tilde{\delta}^T & \tilde{z}^T & \tilde{\omega}^T \end{bmatrix}^T$, the equivalent formulation of the optimal control problem is obtained as follows:

$$\min_{\tilde{V}} \quad C_J^T \tilde{V}, \tag{52}$$

subject to

$$F_1 \tilde{V} \leq F_2 x(1) + f_3 \tag{53}$$

$$F_4 \tilde{V} = F_5 x(1) + f_6 \tag{54}$$

where $C_J = \begin{bmatrix} \Delta s_1 & \cdots & \Delta s_N & 0 & \cdots & 0 & \lambda & \cdots & \lambda \end{bmatrix}^T$. This can be shown as follows. The constraints for the MILP problem (48) are considered for $k = 1, 2, \ldots, N$. We can substitute $x(k)$ in the constraints by using the state equation (47) recursively. The substituted form is obtained as the following expression:

$$\begin{aligned} x(k) = &\Big[\prod_{j=1}^{k-1} A_j\Big] x(1) + \sum_{i=1}^{k-1} \Big[\prod_{j=i+1}^{k-1} A_j\Big] B_i u(i) + \Big[\prod_{j=2}^{k-1} A_j\Big] C_{1,1} \delta(1) \\ &+ \sum_{i=2}^{k-1} \Big[\prod_{j=i+1}^{k-1} A_j\Big] (A_i C_{i-1,2} + C_{i,1}) \delta(i) + C_{k-1,2} \delta(k) \\ &+ \Big[\prod_{j=2}^{k-1} A_j\Big] D_{1,1} z(1) + \sum_{i=2}^{k-1} \Big[\prod_{j=i+1}^{k-1} A_j\Big] (A_i D_{i-1,2} + D_{i,1}) z(i) \\ &+ D_{k-1,2} z(k) + \sum_{i=1}^{k-1} \Big[\prod_{j=i+1}^{k-1} A_j\Big] e_i. \end{aligned}$$

In addition, the end point condition $x(N+1) = [E_{\text{end}} \;\; T]^T$ needs to be considered in (54). Because we know the value of $x(N+1)$, the values of α_m and β_m in (40) are also known. So the state equation at the end point can be written as

$$x(N+1) = A_N x(N) + B_N u(N) + C_{1,N} \delta(N) + D_{1,N} z(N) + e_N$$

where $A_N = \begin{bmatrix} a_N & 0 \\ \Delta s_N(\alpha_{3,N} + \alpha_{m,N+1} a_N) & 1 \end{bmatrix}$, $B_N = \begin{bmatrix} b_N \\ \Delta s_N \alpha_{m,N+1} b_N \end{bmatrix}$, and $e_N = \begin{bmatrix} c_N \\ \Delta s_N(\alpha_{m,N+1} c_N + \beta_{m,N+1} + \beta_{3,N}) \end{bmatrix}$. By properly defining F_1, F_2, f_3, F_4, F_5, and f_6, we can write all these constraints in the form (53) and (54).

The MILP problem (52)-(54) can be solved by several existing commercial and free solvers, such as CPLEX, Xpress-MP, GLPK (see e.g. (Linderoth and Ralphs, 2005; Atamtürk and Savelsbergh, 2005)).

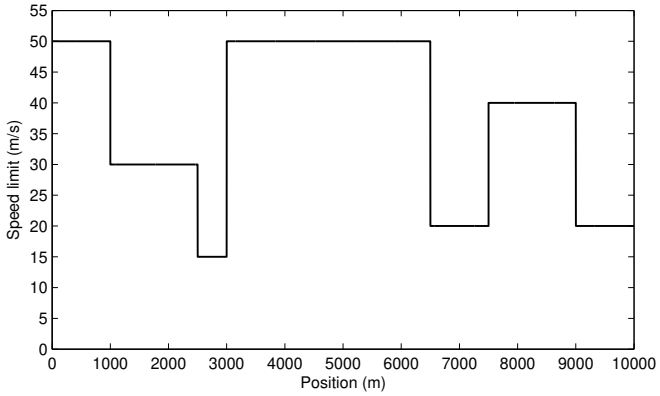

Figure 3: The speed limits along the track

5. Case Study

In order to demonstrate the performance of the pseudospectral method and the MILP approach, we use a case study (inspired by Vašak et al. (2009)) to compare these two approaches to discrete dynamic programming (DDP) approach proposed in (Franke et al., 2002). Franke et al. (2002) evaluated the performance of the coasting strategy obtained by the maximum principle, the sequential quadratic programming approach, and the DDP approach when solving this optimal trajectory planning problem and concluded that DDP yields the best performance.

In the case study of (Vašak et al., 2009), the track length between the departure station and arrival station is 10 km. In Vašak et al. (2009), there were no speed limit and grade profile. We add them as shown in Figure 3 and Figure 4. The rolling stock includes an SBB Re 460 locomotive (Gerber, 2001; Franke et al., 2002; Schank, 2011), whose parameters are shown in Table 1. The rotating mass factor is often chosen as 1.06 in the literature (Hansen and Pachl, 2008) and therefore we also adopt this value. According to the assumption made in Section 2.2, the unit kinetic energy should be larger than zero. In this test case, the minimum kinetic energy is chosen as 0.1 J. The maximum traction force of the SBB Re 460 locomotive is a nonlinear function of the train's velocity and the maximum value of this function is 300 kN as shown in Figure 1. The objective function of the optimal train control problem considered here is a weighted sum of the energy consumption and passenger comfort, where the nominal weight [5] of the passenger comfort is 0.2 in this case study. The total running time for this trip is given by the timetable or the rescheduling process. Here, the total running time given is 450 s, which consists of the minimum running time plus 5% running time supplements. Two cases will be considered here:

- Case A: the maximum traction force is constant.

[5] So we take

$$J = \frac{J_{\text{ec}}}{J_{\text{ec,nom}}} + 0.2\frac{J_{\text{pc}}}{J_{\text{pc,nom}}} \tag{55}$$

where J_{ec} and J_{pc} are the energy consumption and passenger comfort respectively, and $J_{\text{ec,nom}}$ and $J_{\text{pc,nom}}$ are the nominal values of J_{ec} and J_{pc}, which are determined by running the test case study.

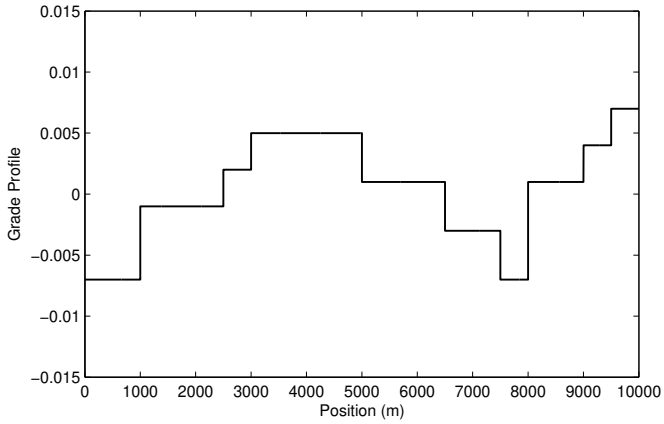

Figure 4: The grade profile of the track

Table 1: Parameters of train and line path

Property	Symbol	Value
Train mass [kg]	m	$5.07 \cdot 10^5$
Basic resistance [N/kg]	R_b	$0.014 + 2.564 \cdot 10^{-5} v^2$
Mass factor	ρ	1.06
Line length [m]	s_T	10^4
Minimum kinetic energy [J]	E_min	0.1
Maximum braking force (regular)[N]	u_min	$-4.475 \cdot 10^5$

- Case B: the maximum traction force is a nonlinear function of the velocity as shown in Figure 1.

5.1. Case A: the maximum traction force is constant

In Case A, just like the case study in (Vašak et al., 2009), we assume that the maximum traction force E_max is constant: $E_\mathrm{max} = 300$ kN. First, the optimal trajectory planning problem is solved using PSOPT (Becerra, 2010a), which implements a pseudospectral method. In this case study, the problem is solved using the Legendre pseudospectral discretizations, with local automatic mesh refinement, starting with 40 nodes.

Second, the problem is solved using the MILP approach. Since the maximum traction force is constant, in this case the linear constraints caused by the PWA constraints (41) of the maximum traction force will not be considered here. In this paper, the PWA approximations of the nonlinear function $f(E) = \frac{1}{2\sqrt{2E}}$ depend on the space interval index k as stated in Section 4.2, i.e. we can have different PWA subfunctions for different space intervals. In Figure 3 there are five speed limits, i.e. 15 m/s, 20 m/s, 30 m/s, 40 m/s, and 50 m/s. Therefore, five different approximations with 2 subfunctions of $f(E)$ are obtained, the parameters of which are given in Table 2. In addition, we introduce two additional PWA approximations of $f(E)$ for the first segment and the last segment. Indeed, since the lowest speed in these two segments is a small positive number

Table 2: The PWA approximations of the nonlinear function $f(E)$

Approx. No.	Segment m	α_m [(s/m)^3]	β_m [s/m]	$E_m - E_{m+1}$ [(m/s)^2]
Approx. 1	Segment 1	$-5.0943 \cdot 10^{-4}$	0.0767	$0.1 - 71.2$
	Segment 2	$-1.7393 \cdot 10^{-4}$	0.0528	$71.2 - 112.5$
Approx. 2	Segment 1	$-3.1153 \cdot 10^{-4}$	0.0665	$0.1 - 115$
	Segment 2	$-6.7188 \cdot 10^{-5}$	0.0384	$115 - 200$
Approx. 3	Segment 1	$-9.4977 \cdot 10^{-5}$	0.0443	$0.1 - 240$
	Segment 2	$-2.3470 \cdot 10^{-5}$	0.0272	$240 - 450$
Approx. 4	Segment 1	$-4.4240 \cdot 10^{-5}$	0.0346	$0.1 - 415$
	Segment 2	$-9.6462 \cdot 10^{-6}$	0.0202	$415 - 800$
Approx. 5	Segment 1	$-1.8122 \cdot 10^{-5}$	0.0251	$0.1 - 640$
	Segment 2	$-6.2127 \cdot 10^{-6}$	0.0175	$640 - 1250$

Table 3: PWA approximations of the nonlinear function $f(E)$ for the first and the last segment

Approx. No.	Segment m	α_m [(s/m)^3]	β_m [s/m]	$E_m - E_{m+1}$ [(m/s)^2]
Approx. 6	Segment 1	$-4.6463 \cdot 10^{-4}$	0.0734	$0.1 - 80.8$
	Segment 2	$-4.6463 \cdot 10^{-4}$	0.0734	$80.8 - 312.5$
Approx. 7	Segment 1	$-1.4458 \cdot 10^{-4}$	0.0534	$0.1 - 229.9$
	Segment 2	$-1.4514 \cdot 10^{-6}$	0.0235	$229.9 - 450$

near zero, a high weight should be given to the low speed interval. The parameters of the PWA approximations for the first and the last segment are given in Table 3.

The length Δs_k for the interval $[s_k, s_{k+1}]$ depends on the speed limits, gradient profile, tunnels, and so on. In addition, if the number of space intervals N is larger, then the computation time of the MILP approach will be longer, but the accuracy will be better. According to the speed limits and grade profile given in Figure 3 and Figure 4, the length of each interval is chosen to equal 500 m, i.e. $\Delta s_k = 500$ m for $k = 1, 2, \ldots, 20$, which provides a good balance between the computation time and the accuracy. As MILP solver, we use CPLEX, implemented through the cplex interface function of the Matlab Tomlab toolbox. For the DDP approach, the continuous nonlinear model of train (11)-(12) is discretized in space. The number of the space intervals is 100 and the length of each space interval is 100 m. To compute the optimal trajectory with DDP, we use a matlab function for dynamic programming that was introduced in (Sundström and Guzzella, 2009).

The optimal solution of the pseudospectral method using PSOPT, which is obtained after 7 mesh refinement iterations, has 179 nodes. The calculation time for PSOPT is 6 min and 10 s on a 1.8 GHz Intel Core2 Duo CPU running a 64-bit Linux operating system and the computation time for DDP is 2 min and 8 s with 100 space intervals as shown in Table 4. However, the calculation time for the MILP approach is 0.32 s on the same CPU and operation system as above, which is

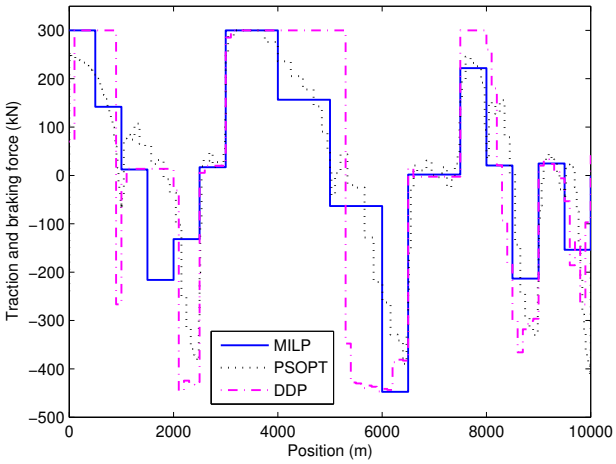

Figure 5: The optimal control inputs with constant maximum traction force for the following approaches: MILP, PSOPT, and DDP

much shorter than the calculation time of PSOPT and DDP.

Figure 5 shows the optimal control inputs with constant maximum traction force, where the dotted line, the solid line, and the dashed line represent the results calculated by PSOPT, MILP, and DDP, respectively. It can be seen from Figure 5 that the results obtained by these three approaches show a similar trend, but there exist more discrete changes but with a smaller magnitude in the control signals of PSOPT and DDP. This is mainly caused by the larger number of space intervals: there are 178 and 100 space intervals in PSOPT and DDP, respectively, but in the MILP approach, there are just 20 space intervals. The optimal control inputs calculated by these three approaches are applied to the nonlinear continuous-time train model (1)-(2). The differential equation of the nonlinear model is solved numerically using a variable step Runge-Kutta method and the obtained speed-position trajectories for the train are shown in Figure 6. The dashed line shows the speed limit for the trip, which is caused by the characteristics of the train, line, etc. The dotted line, the solid line, and the dash-dotted line show the optimal trajectories obtained using control inputs generated by PSOPT, MILP, and DDP, respectively. It can be observed that these optimal trajectories are below the speed limit, which means that the speed constraints are satisfied, i.e. there is no speed limit violation. In addition, we can see from Figure 6 that the optimal trajectories obtained using control inputs generated by PSOPT and DDP are smoother than the one obtained with the MILP approach, which is mainly caused by the number of space intervals as stated before.

In Table 4, the values of the objective function, the computation time, and the constraints violations (i.e. speed limit violation, end position violation, end kinetic energy violation, and end time violation) are compared for the control inputs generated by PSOPT, MILP and DDP applied to the nonlinear continuous-time train model (1)-(2). The values of the objective function obtained by the PSOPT, the MILP, and the DDP approach are 2.424×10^8 and 2.696×10^8, and 2.482×10^8, respectively. The relative differences of the MILP and DDP control performance are 11.2% and 2.4% of that of the pseudospectral method. Therefore, the pseudospectral approach yields the smallest objective value and the constraints violations for the pseudospectral method

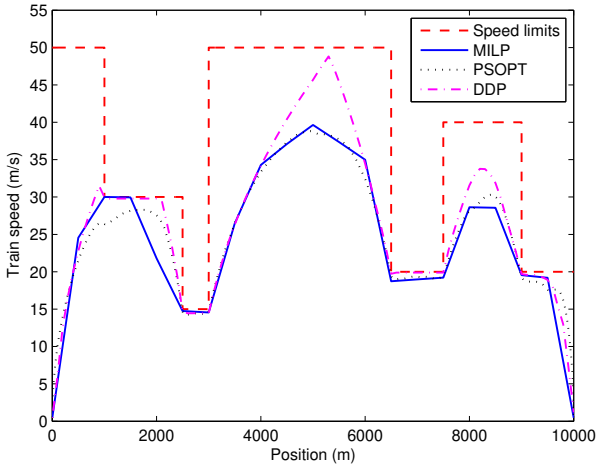

Figure 6: The trajectories generated by the nonlinear continuous-time train model (1)-(2) using optimal control inputs with constant maximum traction force for the following approaches: MILP, PSOPT, and DDP

Table 4: Performance comparison of PSOPT, MILP, and DDP for Case A

	PSOPT	MILP	DDP
$J_{\min}$	$2.424 \cdot 10^8$	$2.696 \cdot 10^8$	$2.482 \cdot 10^8$
CPU time [s]	370	0.32	128
End position s_{end} violation [m]	0	0	0
End kinetic energy E_{end} violation [m/s^2]	0.1	0.005	0.596
End time T_{end} violation [s]	0.496	9.560	6.049
Speed limit violation	No	No	No

are also small. This means the pseudospectral method produces the best performance if the computation time is not considered. But when also considering the computation time and the constraint violations of the end point conditions (i.e. the final position, speed, and running time of the train), the MILP approach provides the best overall performance among the three approaches.

It is worth to note that we apply a trapezoidal integration rule to approximate the time differential equation (12) and then use PWA functions to approximate the nonlinear function (38) in the MILP approach. Therefore, the end time violation in Table 4 of the MILP approach is caused by these approximations. In Wang et al. (2011), where the nonlinear function $f(E) = \frac{1}{2\sqrt{2E}}$ is approximated by the PWA approximation with 3 subfunctions shown in Figure 1, the approximation error of the running time is around 20 s (i.e. around 5% of the total running time). However, in this paper the PWA approximations with 2 subfunctions of the nonlinear function depend on the space interval index k and this results in a reduction of an approximation error of the running time to 10 s (i.e. around 2% of the total running time). Furthermore, we can make the error even smaller by adjusting the PWA approximations according to Footnote 3, but then the CPU time goes up.

Table 5: The coefficients of the varying maximum traction force

Segment j	$c_{1,j}$ [kg · m/s^2]	$c_{2,j}$ [kg/s]	$c_{3,j}$ [kg/m]	$v_j - v_{j+1}$ [m/s]
1	$3.000 \cdot 10^5$	$-1.125 \cdot 10^3$	0	0-22.22
2	$7.263 \cdot 10^5$	$-2.726 \cdot 10^4$	$3.128 \cdot 10^2$	22.22-38.89
3	$4.237 \cdot 10^5$	$-1.120 \cdot 10^4$	$1.000 \cdot 10^2$	38.89-50

Table 6: The coefficients of the PWA approximation of maximum traction force

Segment m	λ_m [kg/m]	μ_m [kg· m/s^2]	$E_m - E_{m+1}$ [(m/s)^2]
1	$-2.9396 \cdot 10^2$	$4.1992 \cdot 10^5$	$0.1 - 500$
2	$-0.9637 \cdot 10^2$	$3.2112 \cdot 10^5$	$500 - 1250$

5.2. Case B: the maximum traction force is a nonlinear function

Now we consider the case with a varying maximum traction force as shown in Figure 1, the coefficients of which according to (3) are listed in Table 5 (Gerber, 2001; Franke et al., 2002; Schank, 2011). In PSOPT, non-smooth path constraints can be handled by introducing a smooth version of the Heaviside function (see Section 3.2). In the MILP approach we need to approximate the nonlinear maximum traction force by PWA functions as shown in (41), whose coefficients also depends on the space interval index k. Here, for simplicity, we just use one PWA approximation with two affine subfunctions for all k. The parameters of the PWA function are listed in Table 6.

Figure 7 shows the optimal control inputs with varying maximum traction force, which is a nonlinear function shown in Figure 1. The dotted line, the solid line, and the dashed line in Figure 7 represent the optimal control inputs obtained using PSOPT, MILP, and DDP, respectively. When we compare Figure 7 to Figure 5, the maximum traction force in Figure 7 is no longer equal to 300 kN for the MILP approach in the space interval $[3000, 4000]$, but it becomes smaller and smaller when the speed grows. This is caused by the varying maximum traction force, which is decreasing when the speed goes up. Similar results can be observed for the optimal inputs calculated by PSOPT and DDP. Figure 8 shows the speed-position trajectories for the train under varying maximum traction force constraints when applying these inputs to the nonlinear train model (1)-(2). The dashed line, the dotted line, the solid line, and the dash-dotted line show the speed limits and the trajectories obtained using control inputs generated by PSOPT, MILP, and DDP, respectively. These trajectories are still below the speed limit, so there is no speed limit violation. In addition, we can see from Figure 8 that the slopes of these three optimal trajectories obtained in the space interval $[3500, 5000]$ are smaller than those of Figure 6, because the maximum traction force is becoming smaller with the increase of the train's speed.

The values of the objective function, the computation time, and the constraints violations are compared for PSOPT, MILP, and DDP in Table 7. Similar as the results in Case A, the pseudospectral approach obtains the minimum objective function value $2.625 \cdot 10^8$ J, which is higher than that in Table 4 (this is due to the inclusion of the constraint of the varying maximum traction force). The relative differences of the MILP and DDP approach in control performance are 7.4% and 2.2% when compared to that of the pseudospectral method. When this problem is solved using PSOPT, with local automatic mesh refinement, starting with 40 nodes, after 7 mesh refinement iterations the final solution obtained has 199 nodes. The calculation time is 19 min

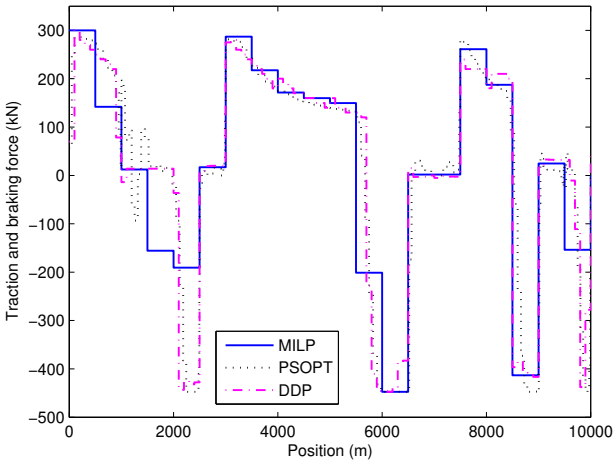

Figure 7: The optimal control inputs with varying maximum traction force for the following approaches: MILP, PSOPT, and DDP

Table 7: Performance comparison of PSOPT, MILP, and DDP for Case B

	PSOPT	MILP	DDP
$J_{\min}$	$2.625 \cdot 10^8$	$2.819 \cdot 10^8$	$2.683 \cdot 10^8$
CPU time [s]	1147	0.54	134
End position s_{end} violation [m]	0	0	0
End kinetic energy E_{end} violation [m/s^2]	0.1	0.005	0.0328
End time T_{end} violation [s]	0	4.170	5.404
Speed limit violation	No	No	No

and 7 s. Compared with the problem in Case A, 20 nodes are added and the computation time is almost 13 min longer. For the DDP approach, the computation time is 2 min and 14 s, which is 6 s longer than that of Case A. In the MILP approach, for each space interval an extra binary variable and an auxiliary real variable are introduced in the MLD model compared with Case A as shown in (46) and (47), since the maximum traction force is considered as a nonlinear function that is approximated by a PWA approximation with 2 subfunctions. Therefore, 40 variables are added to the MILP problem since the number of the space intervals is 20. The computation time is now 0.54 s, which is longer than the 0.32 s in Case A, but it still is much shorter than the pseudospectral method and the DDP approach. Similar to the results shown in Table 4, there are no speed limit violations and the end kinetic energy violation is very small. Furthermore, the end time violation for the pseudospectral method is also very small, but for the MILP and DDP approach this violation is about 1% of the total running time. Therefore, it is concluded that the pseudospectral approach obtains the best control performance, which considers the value of the objective function and the constraints violations. However, when the computation time is also taken into consideration, the MILP approach yields the best overall performance.

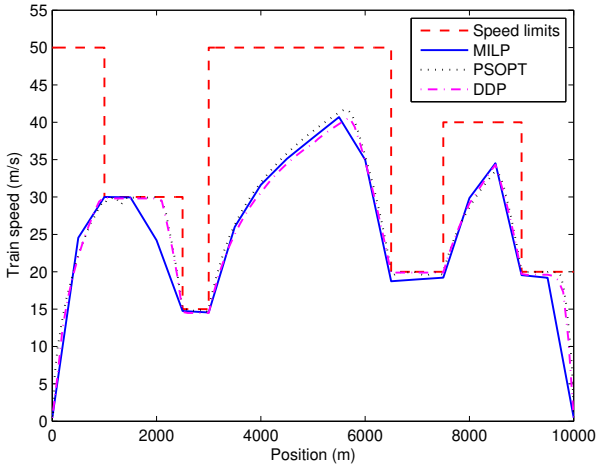

Figure 8: The trajectories generated by the nonlinear continuous-time train model (1)-(2) using optimal control inputs with varying maximum traction force for the following approaches: MILP, PSOPT, and DDP

6. Conclusions and Future Work

In the current paper, the optimal trajectory planning problem for trains is considered. We have proposed two approaches to solve this problem: the pseudospectral method and the mixed integer linear programming (MILP) approach. In the pseudospectral method, the optimal trajectory planning problem is formulated as a multiple-phase optimal control problem based on piecewise line resistance and speed limits. The constraints caused by the varying maximum traction force are defined as nonlinear path constraints. In the MILP approach, the nonlinear train operation model is formulated as a mixed logical dynamical model by using piece-wise affine (PWA) approximations. The variable line resistance (including variable grade profile, tunnels, curves) and speed restrictions are considered, which are included in the constraints of the mixed logical dynamic model. Furthermore, the optimal control problem is recast as an MILP problem, which can be solved efficiently by existing solvers. The case study shows that the pseudospectral method has the best control performance and the MILP has the best overall performance if the computation time is included. In addition, the computation time of the MILP approach is much shorter compared with the pseudospectral method and the discrete dynamic programming approach. The relative difference between the performance of the MILP approach and that of the pseudospectral approach is about 10%.

When the timetable is known, the two approaches proposed in this paper (i.e. the MILP and the pseudospectral approach) can be applied to calculate the optimal trajectory for trains between stations to save energy and to ensure passenger comfort. If there are some disturbances in the network, then one could use a rescheduling approach to reorder trains and determine new timetables (Hansen and Pachl, 2008; D'Ariano et al., 2008). Next, the affected trains have to optimize their trajectories according to the new timetable. In this case, the trajectory planning problem needs to be solved quickly to satisfy the real-time requirements; so then the MILP approach could be applied since it gives the best trade-off between computational speed and accuracy.

An extensive comparison and assessment of the pseudospectral method, the MILP approach, and other approaches in the literature for various case studies and a wide range of scenarios will be a topic for future work. In addition, in this paper we focus on the trajectory planning for a single train between two stations with the assumption that the constraints and disturbances caused by signaling systems and other trains are handled by the lower control level. However, in practice these constraints and disturbances are significant for the capacity of the railway network, and therefore some interesting conflict detection and resolution approaches have been proposed to manage these constraints and disturbances during the rescheduling phases (D'Ariano and Albrecht, 2006; D'Ariano et al., 2007; Corman et al., 2009). In future work, we will combine these conflict detection and resolution approaches with the trajectory planning approaches proposed in this paper to solve the trajectory planning for multiple trains. There we will also use the MILP approach (including hierarchical and distributed optimization if the problem grows too large). Furthermore, the pseudospectral and MILP solvers used in this paper are general-purpose solvers. By making use of the specific structure and properties of the optimal trajectory planing problem, significant speed-ups can be expected. Therefore, in the future we will develop tailored pseudospectral and MILP solvers for the optimal trajectory planing problem for trains.

Moreover, a typical automatic train operation system consists of two levels of control actions. The high-level control is calculating the optimal reference trajectory, as shown in this paper. In the future, we will also focus on the low-level control of the automatic train operation system, which is used to make the train track the pre-planned reference trajectory via certain control methods, such as model predictive control (Camacho and Bordons, 1995), robust control (Green and Limebeer, 1995), and adaptive control (Tao, 1995).

Acknowledgments

The authors thank Sadegh Esmaeil Zadeh from the Delft Center for Systems and Control for discussions about this paper. The authors are also grateful to the reviewers for their helpful comments and many useful suggestions. This research was supported by the European Union Seventh Framework Programme [FP7/2007-2013] under grant agreement no. 257462 HYCON2 Network of Excellence, Chinese Scholarship Council (CSC) grant, the Beijing Municipal Science and Technology Commission (Contract No. D111100000411001), and the State Key Laboratory of Rail Traffic Control and Safety (Contract No. RCS2010ZZ003).

References

Atamtürk, A., Savelsbergh, M.W.P., 2005. Integer-programming software systems. Annals of Operations Research 140, 67–124.

Atkinson, K.E., 1978. An Introduction to Numerical Analysis. John Wiley & Sons, New York, US.

Azuma, S.I., Imura, J.I., Sugie, T., 2010. Lebesgue piecewise affine approximation of nonlinear systems. Nonlinear Analysis: Hybrid Systems 4, 92–102.

Becerra, V.M., 2010a. PSOPT optimal control solver user manual - release 3.

Becerra, V.M., 2010b. Solving complex optimal control problems at no cost with PSOPT, in: Proceedings of IEEE Multi-Conference on Systems and Control, Yokohama, Japan. pp. 1391–1396.

Bemporad, A., Morari, M., 1999. Control of systems integrating logic, dynamics, and constraints. Automatica 35, 407–427.

Bettes, J.T., 2001. Practical Methods for Optimal Control Using Nonlinear Programming. SIAM Series on Advances in Design and Control, Philadelphia.

Betts, J.T., 1998. Survey of numerical methods for trajectory optimization. Journal of Guidance, Control, and Dynamics 21, 193–207.

Bryson, A., Ho, Y., 1975. Applied Optimal Control. Hemisphere (Rev. Printing), New York.
Camacho, E., Bordons, C., 1995. Model Predictive Control in the Process Industry. Springer-Verlag, Berlin, Germany.
Canuto, C., Hussaini, M.Y., Quarteroni, A., Zang, T., 1988. Spectral Methods in Fluid Dynamics. Springer Verlag, New York.
Chang, C., Xu, D., 2000. Differential evolution based tunning of fuzzy automatic train operation for mass rapid transit system. IEE Proceedings - Electric Power Applications 147, 206–212.
Corman, F., A. D'Ariano, D.P., Pranzo, M., 2009. Evaluation of green wave policy in real-time railway traffic management. Transportation Research Part C 17, 607–616.
D'Ariano, A., Albrecht, T., 2006. Running time re-optimization during real-time timetable perturbations, in: Computers in Railways X, WIT Press, Prague, Czech Republic. pp. 531–540.
D'Ariano, A., Pacciarelli, D., Pranzo, M., 2008. Assessment of flexible timetables in real-time traffic management of a railway bottleneck. Transportation Research Part C: Emerging Technologies 16, 232–245.
D'Ariano, A., Pranzoand, M., Hansen, I.A., 2007. Conflict resolution and train speed coordination for solving real-time timetable perturbations. IEEE Transactions on Intelligent Transportation Systems 8, 208–222.
Dielh, M., Bock, H.G., Diedam, H., Wieber, P.B., 2006. Fast direct multiple shooting algorithm for optimal robot control, in: Fast motions in Biomechanics and Robotics Optimization and Feedback Control, Lecture Notes in Control and Information Sciences. pp. 65–94.
Elnagar, G., Kazemi, M.A., Razzaghi, M., 1995. The pseudospectral legendre method for discretizing optimal control problems. IEEE Transactions on Automatic Control 40, 1793–1796.
Fornberg, B., Sloan, D.M., 1994. A review of pseudospectral methods for solving partial differential equations. Acta Numerica 3, 203–267.
Franke, R., Meyer, M., Terwiesch, P., 2002. Optimal control of the driving of trains. Automatisierungstechnik 50, 606–614.
Franke, R., Terwiesch, P., Meyer, M., 2003. An algorithm for the optimal control of the driving of trains, in: Proceedings of the 39th IEEE Conference on Decision and Control, Sydney, Australia. pp. 2123–2128.
Gao, R., 2008. Railway Signal Operation Basis. China Railway Publishing House, Beijing, China.
Gerber, P., 2001. Class re 465 locomotives for heavy-haul freight service. Proceedings of the Institution of Mechanical Engineers. Pt.F. Journal of Rail and Rapid Transit 215, 25–35.
Gill, P.E., Murray, W., Saunders, M.A., 2002. SNOPT: An SQP algorithm for large-scale constrained optimization. SIAM Journal on Optimization 12, 979–1006.
Gong, Q., Kang, W., Bedrossian, N., Fahroo, F., P.Sekhavat, Bollino, K., 2007. Pseudospectral optimal control for military and industrial applications, in: Proceedings of the 46th IEEE Conference on Decision and Control, New Orleans, LA, USA. pp. 4128–4142.
Gong, Q., Ross, I.M., Kang, W., Fahroo, F., 2008. Connections between the covector mapping theorem and convergence of pseudospectral methods for optimal control. Computational optimization and applications 41, 307–335.
Green, M., Limebeer, D.J.N., 1995. Linear Robust Control. Prentice Hall, Englewood Cliffs, US.
Hansen, I., Pachl, J., 2008. Railway, Timetable & Traffic: Analysis, Modelling, Simulation. Eurailpress, Hamburg, Germany.
Howlett, P., 2000. The optimal control of a train. Annals of Operations Research 98, 65–87.
Howlett, P.G., 1990. The optimal strategy for the control of train. Journal of the Australian Mathematical Society. Series B. Applied Mathematics 31, 454–471.
Huerlimann, D., Nash, A.B., 2003. OPENTRACK - Simulation of railway networks, user manual version 1.3. Institute for Transportation Planning and Systems, ETH Zürich.
Ichikawa, K., 1968. Application of optimization theory for bounded state variable problems to the operation of a train. Bulletin of Janpanese Society of Mechanical Engineering 11, 857–865.
Kanwal, R.P., 1983. Generalized Functions: Theory and Technique. Academic Press, New York.
Khmelnitsky, E., 2000. On an optimal control problem of train operation. IEEE Transactions on Automatic Control 45, 1257–1266.
Ko, H., Koseki, T., Miyatake, M., 2004. Application of dynamic programming to optimization of running profile of a train, in: Computers in Railways IX, WIT Press, Southhampton, Boston, USA. pp. 103–112.
Krasemann, J.T., 2012. Design of an effective algorithm for fast response to the re-scheduling of railway traffic during disturbances. Transportation Research Part C: Emerging Technologies 20, 62–78.
Linderoth, J., Ralphs, T., 2005. Noncommercial software for mixed-integer linear programming. Optimization Online .
Liu, R., Golovicher, I.M., 2003. Energy-efficient operation of rail vehicles. Transportation Research Part A: Policy and Practice 37, 917–931.
Mao, B., 2008. The Calculation and Design of Train Operation. People Transport press, Beijing, China.
Midya, S., Thottappillil, R., 2008. An overview of electromagnetic compatibility challenges in European Rail Traffic Management system. Transportation Research Part C: Emerging Technologies 16, 515–534.
Peng, H., 2008. Urban Rail Transit System. China Communication Press, Beijing, China.

Pontryagin, L.S., 1962. The Mathematical Theory of Optimal Processes. Interscience publisher, New York.
Rao, A.V., Benson, D.A., Darby, C., Patterson, M.A., Francolin, C., Sanders, I., 2010. Algorithm 902: GPOPS, a matlab software for solving multiple- phase optimal control problems using the Gauss pseudospectral method. ACM Transactions on Mathematical Software 37, 22:1–22:39.
Rochard, B.P., Schmid, F., 2000. A review of methods to measure and calculate train resistances. Proceedings of the Institution of Mechanical Engineers, Part F: Journal of Rail and Rapid Transit 214, 185–199.
Ross, I.M., 2004. User's manual for DIDO: A MATLAB application package for solving optimal control problems. Tomlab Optimization Inc, Pullman, US.
Ross, I.M., Fahroo, F., 2003. Legendre pseudospectral approximations of optimal control problems, in: Kang, W., Borges, C., Xiao, M. (Eds.), New Trends in Nonlinear Dynamics and Control and their Applications. Springer-Verlag, Berlin. volume 295 of *Lecture Notes in Control and Information Science*, pp. 327– 342.
Ross, I.M., Fahroo, F., 2004. Pseudospectral knotting methods for solving optimal control problems. Journal of Guidance, Control, and Dynamics 27, 397–405.
Rutquist, P., Edvall, M., 2008. PROPT: MATLAB Optimal Control Software. Tomlab Optimization Inc, Pullman, US.
Schank, T., 2011. A fast algorithm for computing the running-time of trains by infinitesimal calculus, in: Proceedings of the 4th International Seminar on Railway Operations Modelling and Analysis RailRome2011, Rome, Italy.
Sundström, O., Guzzella, L., 2009. A generic dynamic programming matlab function, in: Proceedings of the18th IEEE International Conference on Control Applications, Part of 2009 IEEE Multi-Conference on Systems and Control, Saint Petersburg, Russia. pp. 1625–1630.
Tao, G., 1995. Adaptive control design and analysis. John Wiley & Sons, Hoboken, US.
Vašak, M., Baotić, M., Perić, N., Bago, M., 2009. Optimal rail route energy management under constraints and fixed arrival time, in: Proceedings of the European Control Conference, Budapest, Hungary. pp. 2972–2977.
Wächter, A., Biegler, L.T., 2006. On the implementation of a primal-dual interior point filter line search algorithm for large-scale nonlinear programming. Mathematical Programming 106, 25–57.
Wang, Y., De Schutter, B., Ning, B., Groot, N., van den Boom, T., 2011. Optimal trajectory planning for trains using mixed integer linear programming, in: Proceedings of the 14th International IEEE Conference on Intelligent Transportation Systems (ITSC 2011), Washington, DC, USA. pp. 1598–1604.
Williams, H.P., 1999. Model Building in Mathematical Programming (4th ed.). John Wiley & Sons, Chichester, England.